View-based Interpretation of Real-time Optical Flow for Gesture Recognition

Ross Cutler
Univerity of Maryland
College Park, Maryland
rgc@cs.umd.edu

Matthew Turk
Microsoft Research
Redmond, Washington
mturk@microsoft.com

Abstract

We have developed a real-time, view-based gesture recognition system. Optical flow is estimated and segmented into motion blobs. Gestures are recognized using a rule-based technique based on characteristics of the motion blobs such as relative motion and size. Parameters of the gesture (e.g., frequency) are then estimated using context specific techniques. The system has been applied to create an interactive environment for children.

1 Introduction

For many applications, the use of hand and body gestures is an attractive alternative to the cumbersome interface devices for human-computer interaction. This is especially true for interacting in virtual reality environments, where the user is no longer confined to the desktop and should be able to move around freely. While special devices can be worn to achieve these goals, these can be expensive and unwieldy. There has been a recent surge in computer vision research to provide a solution that doesn't use such devices.

This paper describes a real-time vision-based gesture recognition system. Taking a bottom-up, view-based approach, rather than reconstruct the body, we use optical flow to segment the dominant moving body parts (e.g., hands, arms) into "motion blobs." Given the motion blobs and their general characteristics as input, actions are recognized using a rule-based approach. Once an action is detected, parameters of that action (e.g., frequency) are estimated until that action stops.

1.1 Application

Personal computers are widely used as educational tools in grades K-12 and higher. However, for children under the age of five, the keyboard and mouse can be an obstacle for interacting with the computer. We applied our gesture recognition system to create an environment that allows the child to interact with the computer using hand and body gestures. These gestures are used in the following activities:

Figure 1. System

- Playing "Simon Says"
  - Wave arms like a bird
  - Spin to your left/right
  - Touch your toes; reach for the sky
  - Jump up and down
- Conducting music
  - Clapping, waving to create sounds
  - Waving to set a tempo to conduct music
- Walking, running, and flying through a virtual world

Figure 1 shows the system. A standard 266 MHz Pentium II PC is used with a Sony DS-250 digital video camera.

2 Related Work

Research in motion-based recognition has greatly increased in recent years (see [9] for a recent survey). We will describe the most relevant work below.

Becker [6] developed a real-time system to recognize five basic T'ai Chi gestures. The hands and face are tracked using a stereo camera system that tracks skin blobs [3].

The 3D velocity of the hands are used as input to a Hidden Markov Model (HMM) based system. While users can perform each gesture with a different total duration, the velocity of hands are assumed to be approximately the same across users.

Davis and Bobick [10] use a view-based bottom-up approach to gesture recognition. They construct a binary motion-energy image (MEI) which represents where motion has occurred in an image sequence. They also construct a motion-history image (MHI) which is a scalar-valued image where intensity is a function of recency of motion. These view-specific templates are matched against stored models of views of known actions (using moments to provide invariance to scale and translation). Actions are recognized in real-time, but are only invariant to linear changes in speed. This system has been applied to an interactive play-space for children (KidsSpace).

Polana and Nelson [16] recognize periodic motions in an image sequence by first aligning the frames with respect to the centroid of an object so that the object remains stationary in time. Periodic motion is extracted from the graylevel signals using Fourier analysis. A normalization procedure is used to produce a spatio-temporal solid that is invariant to spatial scale, translation, and temporal scale (i.e. frequency). Motion model feature vectors are defined using information from this spatio-temporal solid. The classification is performed using a nearest centroid algorithm.

Black and Yacoob [7] use a rule-based reasoning system to recognize facial expressions of people. The input to the reasoning system are actions such as “inward lowing of brows” and “mouth contracting.” These inputs are determined by tracking patches on the eyes, brows, and mouth.

Wilson and Bobick [19] address the problem of recognizing gestures that exhibit meaningful variations. For example, a pointing gesture requires not only the gesture to be recognized, but the estimated direction of pointing as well. They extend the standard HMM by including a global parametric variation in the output probabilities of the states of the HMM. EM is used to train the parametric HMM.

3 Optical Flow Estimation

An optical flow algorithm estimates the 2D flow field from image intensities. While many techniques have been developed, accurate and dense estimates are difficult to achieve (see [5] for a recent survey). There are four general categories for optical flow algorithms: differential (gradient), region-based matching, energy-based, and phased-based. Differential techniques compute velocity from spatiotemporal derivatives (or filtered version of the image). Region-based techniques compare patches of the image (or filtered image) at different disparities to determine the flow. Energy and phase-based methods apply velocity-tuned filters on the image sequence and extract the velocities from the filters' output. In a comparison of these four techniques, Barron et. al [4] found the phase-based approach of Fleet and Jepson [12] to be the most accurate; unfortunately, it is also the slowest [15].

For view-based gesture recognition, our requirements for an optical flow algorithm are as follows:

- produce dense flow
- accuracy: direction within 25°, magnitude within 50%
- able the work on large disparities (e.g., 15 pixels)
- tolerant to noise
- usable on interlaced and decimated images
- efficient; parallizable; real-time (30 Hz) on 160x120 images
- functional in low-contrast environments

Dense flow is desirable since it has redundancy in data that allows for better performance and robustness. Note that the required accuracy is not great. This is mainly a tradeoff for speed, but we have found that these requirements are sufficient for our segmentation algorithm and recognition analysis.

We make the following assumptions about our environment:

- relatively static background
- illumination changes slowly

As noted in [4], region-based matching techniques (e.g., correlation-based) are more robust to noise than differential techniques. In addition, region-based techniques work well even when the input is interlaced or decimated. Camus [8] notes that correlation-based techniques are also less sensitive to illumination changes between frames than differential based techniques.

Computing optical flow in real-time has traditionally been done using expensive hardware (e.g., DSPs or field-programmable gate arrays). However, general purpose CPUs are now becoming available with Single-Instruction, Multiple Data (SIMD) instructions (e.g., Intel Pentium II, Sun UltraSparc). For this system, we used a 266 MHz Intel Pentium II PC. Our MMX implementation of the algorithm flow algorithm produced a 400% increase in speed (compared to non-MMX optimized code), which was critical in making the system real-time.

We choose to use a correlation-based algorithm to estimate the optical flow, using the sum of absolute differences (SAD) instead of correlation for efficiency reasons. A major drawback to correlation-based algorithms is that they can be computationally expensive. Consider an image of size $I \times I$, a patch radius of P, and a search radius of R. We define a similarity metric D on the images I_1 and I_2 for the pixel (x, y) and disparity (dx, dy) as:

$$D(x,y,dx,dy) = \sum_{i=-P}^{P}\sum_{j=-P}^{P} E$$

where

$$E = \mid I_1(x+i, y+j) - I_2(x+i+dx, y+j+dy) \mid$$

To determine the flow between images I_1 and I_2 at a point (x,y) we minimize $D(x,y,dx,dy)$ for $(dx,dy) \in \{[-R,R] \times [-R,R]\}$. A straightforward implementation of this algorithm would require $O(I^2 P^2 R^2)$ pixel comparisons. However, there are redundant comparisons in this technique, and by storing intermediate results we can reduce the complexity to $O(I^2 R^2)$ [11]. Note that although we have reduced the computational complexity, we have increased the required memory bandwidth, as intermediate results must be stored in memory. For this technique to give an overall time savings, we must have a fast memory system. Unfortunately the currently available Pentium II systems do not have sufficient memory bandwidth to make this technique feasible. That is, the memory bottleneck is so severe that it overrides the reduction in complexity, and so we instead implement the more computationally expensive algorithm.

In order to satisfy the requirement that our flow algorithm work well in low contrast conditions, we use color (in YUV[1].) to define our similarity metric:

$$D'(x,y,dx,dy) = \sum_{i=-P}^{P}\sum_{j=-P}^{P} E_Y + E_U + E_V$$

where

$$E_C = \mid I_{1C}(x+i, y+j) - I_{2C}(x+i+dx, y+j+dy) \mid$$

We found that using YUV color in this way gave significantly better flow estimates than simply using the grayscale image data. In particular, color helps to distinguish the hand in front of the face, even though both objects have similar grayscale values.

3.1 Motion Detection

If we assume that the background is relatively static, then we can reduce optical flow computation time by only computing the flow for pixels that satisfy a motion detection criterion. Specifically, we compute the temporal derivative of a Gaussian smoothed image I_t^* and threshold it by the value $K\sigma$, where σ is the average standard deviation of the white noise in the video system for the YUV color channels (measured off-line), and K is a constant (typically 4). We compute the flow at pixel (x,y) only if $M(x,y) = 1$, where

[1]The YUV color space was used since the Sony DS-250 camera outputs YUV:422 data. The RGB color space was found to give similar results.

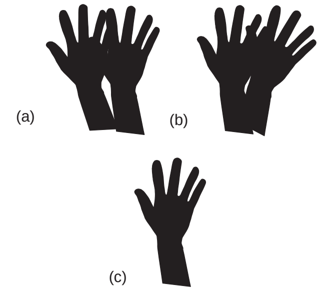

Figure 2. Mask applied to a hand moving left to right. Let A,B, and C be the hand at time $t-1$, t, and $t+1$, respectively. (a) $M(x,y,t-1) = A \vee B$); (b) $M(x,y,t) = B \vee C$; (c) $M'(x,y,t) = B$

$$M(x,y,t) = \begin{cases} 1 & \text{if } E_Y^* + E_U^* + E_V^* > K\sigma \\ 0 & \text{otherwise} \end{cases}$$

where

$$E_C^* = \mid I_{1C}^*(x,y) - I_{2C}^*(x,y) \mid$$

The Gaussian smoothing serves two purposes: first, it reduces the noise inherent in the images. Second, it gives a support patch from which we compare the change in motion from (that is, we are comparing the motion for a patch instead of a single pixel).

$M(x,y,t)$ can be improved by using three sequential images instead of two in the following way:

$$M'(x,y,t) = M(x,y,t-1) \wedge M(x,y,t)$$

While $M(x,y,t) = 1$ if pixel (x,y) is moving in image I_t or I_{t+1}, $M'(x,y,t) = 1$ only if (x,y) is moving in I_t (see Figure 2). This further reduces the number of pixels to compute the flow on. Moreover, it also eliminates the problem of computing the flow of a pixel (x,y) in I_t which is occluded in I_{t+1} (e.g., (x,y) is on on the leading edge of a moving object).

Note that $M'(x,y,t)$ (and $M(x,y,t)$) will filter out moving regions that have little texture. This is very desirable, as these regions will produce inaccurate flow estimates.

3.2 Flow Estimate Confidence Measures

There are many ways to estimate the confidence in the flow estimate. For example, Anandan [1] fits a cubic surface to the SSD values and defines a confidence measure based

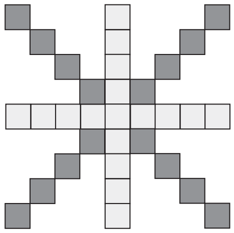

Figure 3. Search pattern

on the curvatures of this surface. Another way to verify that the flow is correct is to use the left-right check [11]; that is, compute the flow for image I_t with respect to I_{t+1}, then repeat for I_{t+1} with respect to I_t. Only the flow estimates that are the same (or nearly so) should be used.

While both of these techniques give good results, they are also are computationally expensive. Instead, we simply rely on the motion mask $M'(x, y, t)$ to eliminate the two most common flow estimate errors, namely occlusion boundaries and low texture areas. We find this technique to give a sufficiently good flow estimate for our later analysis.

3.3 Search Pattern

To determine the flow between images I_1 and I_2 at a point (x, y) we minimize $D'(x, y, dx, dy)$ for $(dx, dy) \in [-R, R] \times [-R, R]$. However, Ancona and Poggio [2] shows that the 1D search pattern $(dx, dy) \in [-R, R] \times \{0\} \cup \{0\} \times [-R, R]$ gives a reasonable approximation to the full 2D search pattern. The advantage to the 1D search space is it is much less computationally expensive. We utilize this in our algorithm, adding the diagonals to the search pattern (see Figure 3). Our tests show that this 1D search pattern gives good results with our data sets for disparities $D \leq 15$.

4 Optical Flow Segmentation

In order to analyze the optical flow at a higher level, we first segment it into "motion blobs." There are many ways to segment optical flow (e.g., [14], [18], [17]). However, we are constrained in choosing a technique that works with inaccurate flow and will run in real-time. We use the K-means algorithm [13] to segment the flow, using a feature vector $v = (x, y, \theta)$, where θ is the direction of the flow vector (u, v) at pixel (x, y). The distance metric used in the K-means algorithm is:

$$S(x, y, \theta) = \frac{\mid x - \bar{x} \mid}{\frac{|\bar{x}| + |x|}{2} + \sigma_x} + \frac{\mid y - \bar{y} \mid}{\frac{|\bar{y}| + |y|}{2} + \sigma_y} + \frac{\mid \theta - \bar{\theta} \mid}{\frac{|\bar{\theta}| + |\theta|}{2} + \sigma_\theta}$$

where $(\bar{x}, \bar{y}, \bar{\theta})$ is the cluster's centroid and $\sigma_x, \sigma_y, \sigma_\theta$ are on the order of the error estimates of x, y, θ, respectively. We are using a constant flow direction model. The magnitude is not used as it will change for rotational motions. While an affine flow model would handle rotational motions, it is currently too computationally expensive. The constant flow direction model is sufficient for out current gestures and environment assumptions.

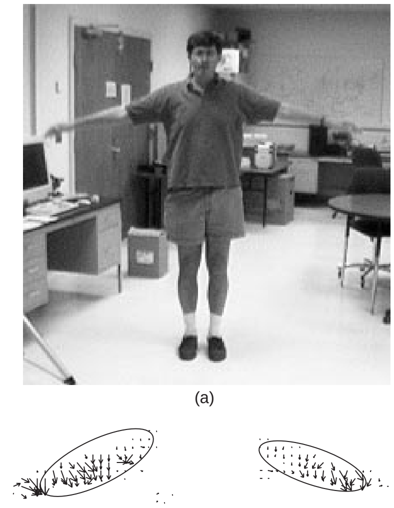

(a) (b)

Figure 4. (a) Flapping action; (b) Flapping flow and segmented motion blobs

The blobs are modeled as a best fitting ellipse for the flow vector locations (x, y) in each cluster; the flow direction or magnitude is not used to compute the best fitting ellipse.

The K-means algorithm assumes we already know the number of clusters. As we will see in the next section, our actions can be modeled with only one or two motion blobs (clusters), so we run our segmentation algorithm for both number of blobs and input the results to the gesture recognition system.

See Figure 4 and Figure 5 for examples of the segmented flow.

5 Gesture Recognition and Parameter Estimation

Our view-based approach to gesture recognition uses a rule-based technique to identify an action based on a set of conditions. The following information about the motion blobs are used as input to the action predicates: the number of blobs; the motion of blobs (horizontal, vertical, or rotational); the relative motion between blobs (opposing or same direction); whether the motion is periodic; and the relative size of the blob(s) (the blob's major axis length divided by the user's height (in pixels)). The conditions for

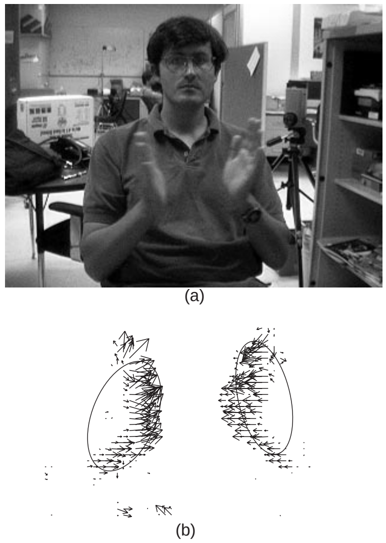

Figure 5. (a) Clapping action; (b) Clapping flow and segmented motion blobs

Action	# of Blobs	Motion	Relation	Cyclic	Size
spinning	1	horiz.	NA	no	0.8
waving	1	rot.	NA	yes	0.2
jumping	1	vert.	NA	yes	0.8
clapping	2	horiz.	oppose	yes	0.2
drumming	2	vert.	oppose	yes	0.4
flapping	2	rot.	same	yes	0.8
marching	2	vert.	oppose	yes	0.4

Table 1. Action conditions

the seven actions in our interactive environment are given in Table 1. These conditions must be satisfied over N consecutive frames, where N is typically about 10. The cyclic condition is determined by Fourier analysis of the motion blob's centroid and major-axis direction. Figure 6 shows the ideal motion blobs for these actions.

Once an action is recognized, the system will go into a mode specific to that action, estimating that action's parameters until the action ceases. For example, the waving action, which consists of the user waving his hand (as in conducting music), estimates the frequency of movement (i.e. the tempo). The frequency is determined by detecting the zero-crossings of the average flow magnitude for the motion blob, which is shown in Figure 7. These zero-crossings correspond to the left- and right-most movements in the waving action, and are labeled as the left and right beat. The time intervals between the left and right beat are averaged over several intervals and inverted to obtain the

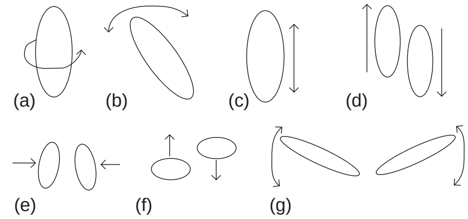

Figure 6. Action motion blobs: (a) spinning, (b) waving, (c) jumping, (d) marching, (e) clapping, (f) drumming, (g) flapping

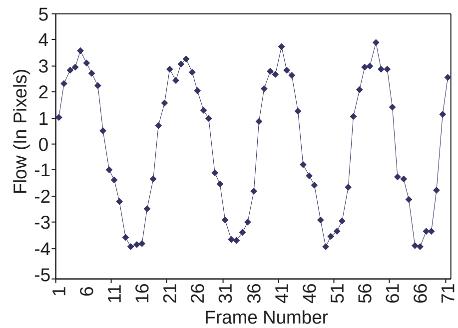

Figure 7. Waving average flow magnitude

frequency. This frequency, along with the left and right beat and the maximum average flow can be used as input to control an interactive environment. The events and parameters for the other actions (see Table 2) are computed in a similar fashion.

6 Results

In order to test our gesture recognition system, we have developed an interactive environment for children. The opening screen for this system displays seven animated characters performing the seven actions in Table 1. If the child wants to conduct music, he or she mimics the ani-

Action	Events	Parameters
spinning	NA	direction, velocity
jumping	up/down	height, velocity
waving	left/right beat	frequency, velocity
clapping	contact	frequency, velocity
drumming	left/right beat	frequency, velocity
flapping	up/down	frequency, velocity
marching	L/R foot up/down	frequency, velocity

Table 2. Action events and parameters

Figure 8. Conducting mode

mated character that is conducting music. Once the action is recognized, the system goes into a conducting mode, shown in Figure 8. In this mode, the user can set the tempo of a song by the frequency of the hand; the left and right beats can be used to progress (incrementally) through the notes in a song. After the user stops waving, the starting screen returns to offer more activities from which to choose.

We have informally tested this system with both children and adults. Participants have found it to be fun, intuitive, and compelling. The immediate feedback of the musical sounds and animated characters is engaging, especially for children. (After using it at the lab, the young son of one of the authors couldn't understand why his home computer wouldn't do the same thing for him!) Some people tended to prefer certain actions, while others enjoyed switching among all of them. Because the recognition is based on optical flow estimation, there are few constraints regarding clothing, the background scene, etc.; people can move the camera, change the lighting conditions, move around somewhat while gesturing, and allow others to be in the scene (if they're not moving much).

7 Conclusions

We have used real-time optical flow to segment a user's dominant motions. Using a rule-based technique and general characteristics of the motion blobs, we can recognize among a set of gestures. The parameters for each gesture are estimated in a context specific manner. The system has been successfully applied to an interactive system for children. Future work for this system includes: adding more gestures (e.g., pointing) and allowing simultaneous gestures (e.g., clapping while marching); using fuzzy logic for the reasoning system to make the gesture recognition more robust; enhancing the motion segmentation to allow intersecting motion blobs; and adding the ability to handle multiple users in the field of view, with associated gestures for interaction (e.g., shaking hands).

References

[1] P. Anandan. A computational framework and an algorithm for the measurement of visual motion. *International Journal of Computer Vision*, 2:283–310, 1989.

[2] N. Ancona and T. Poggio. Optical flow from 1D correlation: Application to a simple time-to-crash detector. Technical Report AI Memo 1375, MIT AI Lab, 1993.

[3] A. Azarbayejani and A. Pentland. Real-time self-calibrating stereo person tracking using 3-D shape estimation from blob features. Technical Report 363, MIT Media Lab Perceptual Computer Section, 1996.

[4] J. Barron, D. Fleet, S. Beauchemin, and T. Burkitt. Performance of optical flow techniques. In *Proceedings of the Computer Vision and Pattern Recognition*, pages 236–242, 1992.

[5] S. S. Beauchemin and J. L. Barron. The computation of optical flow. *ACM Computing Surveys*, 27(3):433–467, 1995.

[6] D. A. Becker. Sensei: A real-time recognition, feedback and training system for t'ai chi gestures. Master's thesis, MIT Media Lab Perceptual Computer Section, 1997.

[7] M. Black and Y. Yacoob. Tracking and recognizing facial expressions in image sequences, using local parameterized models of image motion. Technical Report CAR-TR-756, University of Maryland, College Park, 1995.

[8] T. Camus. Real-time quantized optical flow. *Journal of Real-Time Imaging*, 3:71–86, 1997.

[9] C. Cedras and M. Shah. Motion-based recognition: A survey. *Image and Vision Computing*, 13(2):129–155, 1995.

[10] J. W. Davis and A. F. Bobick. The representation and recognition of action using temporal templates. Technical Report 402, MIT Media Lab Perceptual Computer Section, 1996. Also appears in CVRP 1997.

[11] O. D. F. et al. Real time correlation based stereo: algorithm, implementations and applications. Technical Report 2013, INRIA, 1993.

[12] D. Fleet. *Measurement of Image Velocity*. Kluwer Academic Publisher, Norwell, 1992.

[13] A. Jain and R. Dubes. *Algorithms For Clustering Data*. Prentice-Hall, 1988.

[14] A. Jepson and M. Black. Mixture models for optical flow computation. Technical Report RBCV-TR-93-44, Univerity of Toronto, 1993.

[15] H. Liu, T.-H. Hong, M. Herman, and R. Chellappa. Accuracy vs. efficiency trade-offs in optical flow algorithms. In *European Conference on Computer Vision*, pages 174–183, 1996.

[16] R. Polana and R. Nelson. Recognizing activities. In *International Conference on Patern Recognition*, 1994.

[17] H. Sawhney and S. Ayer. Compact representation of videos through dominant and multiple motion estimation. *IEEE Transactions on Pattern Analysis and Machine Intelligence*, 18(8):814–830, 1996.

[18] J. Y. A. Wang and E. H. Adelson. Representing moving images with layers. Technical Report 279, MIT Media Lab Perceptual Computer Section, 1994.

[19] A. Wilson and A. Bobick. Recognition and interpretation of parametric gesture. Technical Report 421, MIT Media Lab Perceptual Computer Section, 1997.